Bridge Safety, Maintenance, Management, Life-Cycle, Resilience and Sustainability – Casas, Frangopol & Turmo (eds)
© 2022 copyright the Author(s), ISBN 978-1-032-35623-5

The effectiveness of viscous dampers in the seismic retrofitting project of an Italian cantilever bridge

A. Lupoi
Sapienza University of Rome, Italy

A. Greco
Studio Speri Società di Ingegneria S.r.l. , Rome, Italy

ABSTRACT: The viscous anti-seismic devices, also called "*viscous dampers*", are frequently used to improve the seismic response of structures and in particular of bridges. Unlike other anti-seismic devices, the *viscous dampers* are characterized by a considerable damping and yield capacity which allows to dissipate a rate of energy induced by the seismic action and to contain, together with the displacements, also the stresses that arise in the structural elements. Due to their performance characteristics, the *viscous dampers* have been used within a huge seismic retrofitting project of an Italian bridge located on A14 highway Bologna-Taranto in the Abruzzo Region, which is the case study outlined in this paper.

1 INTRODUCTION

This paper mainly focuses on the seismic retrofitting project of an Italian cantilever bridge realized with viscous damper devices, the use of which allowed to be in compliance with the safety factors required by Italian technical standards [8] – both for the bridge piers' capacity and for the maximum capacity of the shear keys' excursion interposed between the spans. This latter aspect has been the primary criticality identified by tests carried out in *ante operam* configuration.

From numerical point of view, given the typical non-linear behavior of viscous dampers, the response of the bridge has been assessed using a direct-integration time-history nonlinear analysis with the finite element model. Moreover, due to the considerable length of the bridge, the spatial variability of seismic ground motion has been also considered and, consequently, the implementation of asynchronous time histories at the base of each pier of the bridge.

Following the explanation of all such assumptions adopted for this project, the design of the bridge, its seismic response as well as the criticalities emerged from the analysis performed in the *ante operam* phase, are describe in the next chapters. Finally, the interventions' detail, the design criteria, the performed analysis and the relative results, in relation to the aims of the seismic retrofitting project, are explained.

2 DESIGN OF THE BRIDGE

The bridge overpasses a river flowing through a wide valley, and it is located on Italian highway.

Figure 1. Sud-Est view of the Bridge.

The bridge was built in 1973 and it can be deemed an imposing work of great architectural value as well as a massive engineering structure. The bridge is 860 m long and consists of eight (8) large spans with separate carriageways: the six internal spans are 112,5 m long while the two external ones are 65 m long.

The single deck, of 9.8 m width (8.8 m for driveways), is erected with the *balanced cantilever method* starting from the piers and cantilevering out from both sides by the construction of successive

DOI: 10.1201/9781003322641-321

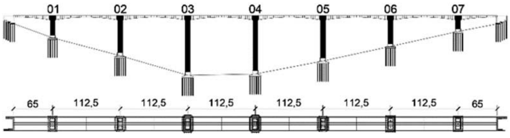

Figure 2. Vertical and horizontal sections of the bridge.

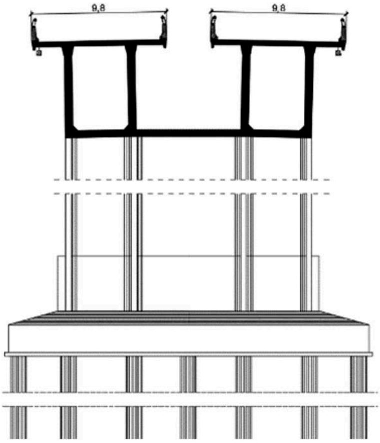

Figure 3. Transverse section of the bridge.

precast segments. The decks are connected to each other by steel shear keys, the function of which is to prevent the relative vertical displacements only.

Each internal half span, with a parabolic bottom profile (from 7 m to 2,3 m), is assembled by 14 segments with a concrete box section of R_{ck} 50 MPa. However, the external spans are assembled by 17 segments. The prestressing system of the decks consists of 42ϕ7 BBRV cables with a ultimate tensile strength f_{ptk} and yield tensile strength $f_{p(0.1)k}$ equal to 1650 MPa and 1450 Mpa, respectively.

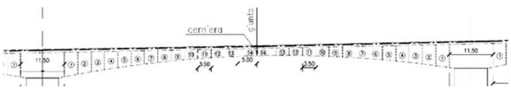

Figure 4. Typical span of the bridge.

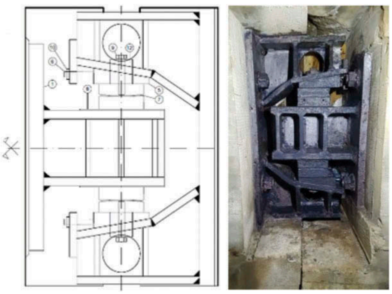

Figure 5. Shear keys currently installed on the bridge.

The piers and foundations are in ordinary reinforced concrete, with a cubic resistance of R_{ck} 40 MPa and 35 MPa, respectively.

Pier stems are characterized by a box section and by a variable height ranging from 13 m to 90 m. Foundations piles are 30 m long with a ϕ1200 diameter.

3 CRITICAL ISSUES IN "ANTE-OPERAM" CONFIGURATION

The requirement of the seismic retrofitting of the bridge has emerged from the assessment of the seismic response in the original configuration. The analyses showed the inadequacy of the shear keys in terms of the maximum excursion of 150 mm, to (i) absorb the displacements induced by the seismic action and, (ii) prevent the pounding effect between adjacent spans and/or their loosening when counter-phase of the piers occur. It is worth noting that the bridge was not designed for the seismic action in the original project.

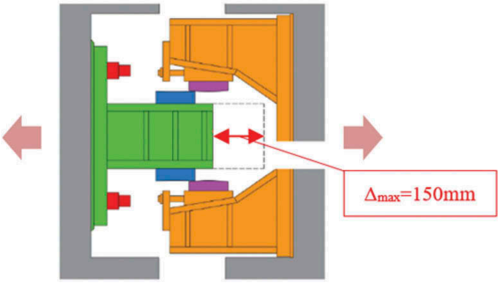

Figure 6. Loosening of shear keys, currently installed on the bridge, due to a counter-phase of the piers.

During the *"ante operam"* phase, the dynamic response of the structure is captured by seven finite element models faithfully representing each one of the piers. A modal response spectrum analysis is carried out for each independent model.

Once periods, vibration modes and seismic displacements (Figure 8 and Table 1) of the seven top piers are obtained, the maximum excursions (Δ) at the joints between adjacent spans are computed as

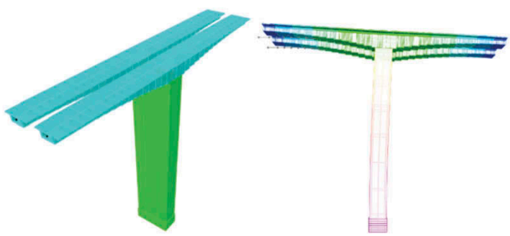

Figure 7. FE model and first modal form of a pier.

Table 1. Fundamental periods, accelerations and displacements response spectra of the piers at the collapse limit state.

PIER	H (m)	T1 (s)	S_e (g)	S_d (mm)
1	26,53	1,16	0,475	159
2	49,88	1,74	0,317	238
3	81,33	3,11	0,153	367
4	79,18	3,00	0,164	367
5	58,73	2,07	0,266	284
6	36,58	1,34	0,411	184
7	13,03	1,03	0,535	141

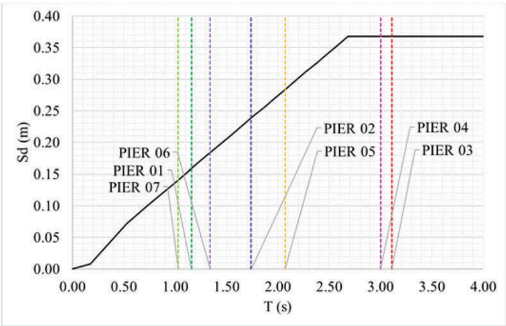

Figure 8. Displacement response spectra of the piers at the collapse limit state.

required by §7.2 of the Ministerial Decree dated 17/01/2018, comparing with the excursion capacity of the original shear keys, equal to 150 mm.

$$\Delta = d_{Eg} + d_{Es}$$

where:

- $d_{Es} = 1,25\ (d_{Es,i}^{2} + d_{Es,j}^{2})^{0,5}$
- $d_{Eg} = d_{ij}(x) = d_{ij,max} - d_{ij0}\ (1 - e^{-1,25(x/vs)^\wedge 0,7})$
- $d_{ij,max} = 1,25\ (d_{gi}^{2} + d_{gj}^{2})^{0,5}$
- $d_g = 0,025 \cdot a_g \cdot S \cdot T_C \cdot T_D$
- $x = 112,5$ m
- $v_s = 270$ m/s

Table 2 summarizes the maximum excursions of the expansion joints got from the analysis: values are greater than the sliding mechanism of the original shear keys which are therefore they are inadequate.

However, with reference to the safety checks related to the capacity of the structural elements, no critical issues are raised. In fact, the capacity/demand ratios are in general higher than one, except for the shear ratio of the shortest stems equal to 0.82 due to the greater stiffness and lower axial load. This value, although lower than one, is higher than the admissible limit, equal to 0.8, as provided by Italian technical standards [8] for existing structures.

Table 2. Maximum excursions of the shear keys.

JOINTS	d_{Es} (mm)	d_{Eg} (mm)	Δ (mm)
1: ABUTMENT -PIER 1	159	95	254
2: PIER1- PIER 2	358	127	485
3: PIER 2- PIER 3	547	127	674
4: PIER 3- PIER 4	649	127	776
5: PIER 4- PIER 5	580	127	707
6: PIER 5- PIER 6	422	127	549
7: PIER 6- PIER 7	289	127	416
8: PIER 7-ABUTMENT	141	095	236

4 THE SEISMIC RETROFITTING PROJECT OF THE BRIDGE

4.1 *Objectives and description of the structural measures*

The seismic retrofitting of the bridge is part of the wider consolidation project, including geotechnical and structural measures.

From a geotechnical perspective, landslides movements of the north side of the bridge valley are observed, which involve the abutment and the first piers of the bridge. These landslides activity have caused the closure of the first five joints between decks by preventing their thermal expansion and thus jeopardizing the proper functionality of the structure.

Therefore, the consolidation project initially envisaged the execution of certain geotechnical interventions throughout the use of adequate drainage systems aimed at stabilizing the north side of the valley affected by landslides. Then, structural interventions with the purpose of functionally restoring the bridge and adapting it for the seismic action were planned. This last category of interventions are the subject matters of this paper.

For sake of clarity, the structural interventions planned for this project are:

i. *Reopening of the closed joints no. 2, 3, 4 and 5 up to 32 cm in order to allow the thermal expansions and avoid an unforeseen thermal stress of the deck;*
ii. *Expansion of the joints no. 1, 6, 7 and 8, up to 32 cm (the initial amplitude was 10 cm) in order to take the seismic action by avoiding the pounding effect;*
iii. *Replacement of the shear keys, installed between the joints, with the new ones characterized by a greater excursion capacity (30 cm) in order to take the seismic action by avoiding the their loosening;*
iv. *Seismic retrofitting of the bridge by installation of viscous dampers astride the joints between the decks and between the decks and the abutments. The installation of viscous dampers is*

important to reduce the displacements and the stresses of the piers and, consequently, the excursion of the shear keys;

v. *Installation of a steel transversal restraint to prevent relative displacements between adjacent decks.*

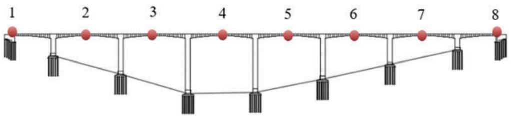

Figure 9. Location of structural measures.

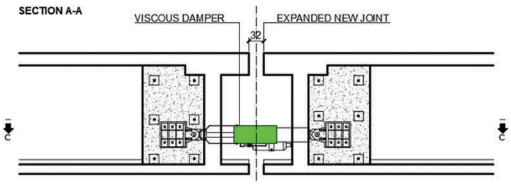

Figure 10. Project configuration: overview of deck vertical section - Installation of viscous damper between the joints expanded up to 32 cm.

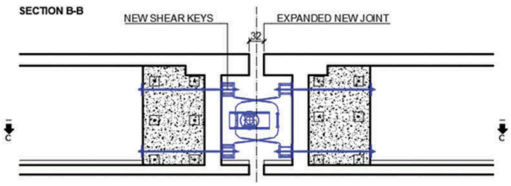

Figure 11. Project configuration: overview of deck vertical section - Installation of new shear keys.

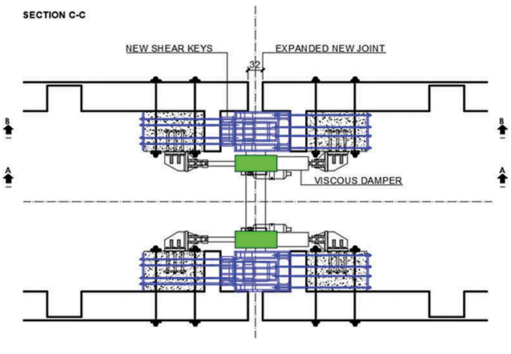

Figure 12. Project configuration: overview of deck horizontal section – New shear keys and viscous dampers.

4.2 *The choice of viscous damper devices*

Design choices are focused on the adoption of viscous damper devices. Among all the available kind of anti-seismic devices, viscous dampers have been the more suitable option for this huge project since they allow the limitation of both stresses and displacements of the structure due to their considerable dissipative property.

The main goal of this seismic retrofitting project is the limitation of the excursions of the joints between the decks, avoiding the absorption of the seismic action by the shortest and stiffest lateral piers.

From an operational perspective, a viscous damper consists of a piston sliding in a cylinder, filled with silicone or any other kind of oil (Figure 13). The piston has a series of small orifices through which the fluid flows, in order to dissipate the energy.

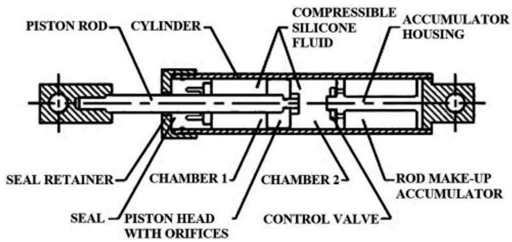

Figure 13. Structural arrangement of viscous damper.

The law governing performance of viscous damper devices is well known in the literature and it is outlined below [1]:

$$F = C\, v^{\alpha}$$

where:

- F= force
- C = damping constant
- v = velocity of piston relative to cylinder
- α = exponent

With respect to the viscous dampers, the exponent α is < 1, variable between 0,015 and 1. The typical trend of the devices' behavior is shown in the figure below (Figure 14).

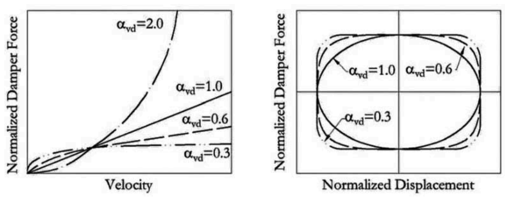

Figure 14. Typical response diagram Force/Velocity (left) and Force/Displacement (α variable from 2 to 0,03).

The diagram shown in Figure 14 establishes the performance of a *viscous damper*. The parameters of the curve can be set by the designer according to the specific requirements.

4.3 *Design of viscous damper*

The design of the viscous dampers' devices is carried out in sequential phases.

The first phase includes a preliminary design a simplified methods based on the inertia forces acting on each pier of the bridge. The adoption of this approach has allowed to select some preliminary viscous dampers in order to verify the feasibility of the interventions with regard to the geometric dimensions.

The second phase has been characterized by detailed design of the viscous dampers *system* based on the interactions between them. The abovementioned phase is carried out, as usual, by iterative procedure aimed at identifying the configuration of devices, with regard to both their position in the bridge and to their target force.

The iterative approach had been also necessary due to the different stiffnesses of each pier.

A unique optimal configuration of devices has been identified through the iterative procedure, which details are summarized in Table 3 and Figure 15. The parameter v* is the velocity at maximum force while the parameter *s* is the maximum excursion of the devices.

Details related to the F.E. model adopted for the performance of the seismic analyses are outlined in §4.4.

Table 3. The viscous dampers used in the project.

JOINT	F (kN)	C [kN/(m/s)^2]	v* (m/s)	s (mm)
1: ABUTMENT - PIER 1	1'500	1'534	0,8	+/-300
2: PIER 1- PIER 2	1'500	1'534	0,8	+/-300
3: PIER 2- PIER 3	2'000	2'045	0,8	+/-250
4: PIER 3- PIER 4	2'500	2'556	0,8	+/-200
5: PIER 4- PIER 5	2'500	2'556	0,8	+/-200
6: PIER 5- PIER 6	2'000	2'045	0,8	+/-250
7: PIER 6- PIER 7	1'500	1'534	0,8	+/-300
8: PIER 7-ABUTMENT	1'500	1'534	0,8	+/-300

4.4 *F.E. model and analysis*

The dynamic response of the bridge in the project configuration is determined by a FE model managed with the support of the SAP2000 code (Figure 16).

Decks, piers and foundation piles are modelled with frame elements [6], [7]; only for the piers is take into account the non-linear constitutive law for the stress-strain relationship of the materials, using the fiber sections with plastic hinges. The soil-structure interaction is evaluated with equivalent soil horizontal "springs" stiffness, in accordance with Reese and Matlock theory (1956).

The presence of the shear keys and the transversal restraint are modelled with *link 2-joint* between adjacent decks. The stiffness of such *link* is previously calibrated for each active degrees of freedom.

The viscous dampers interposed between contiguous decks and connected to them, instead, are modelled with *exponential Maxwell damper links*. Such

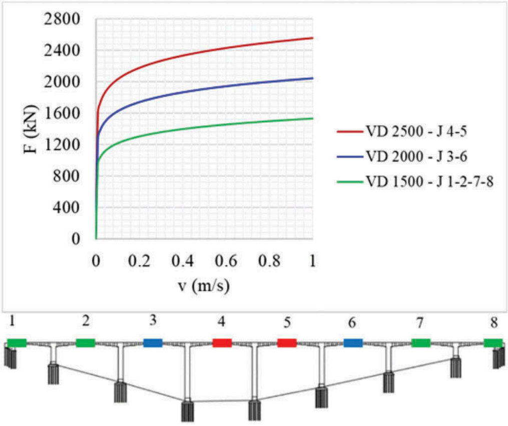

Figure 15. Diagram Force/Velocity of *viscous* damper (above), Placement of *viscous dampers* into the structure (bottom).

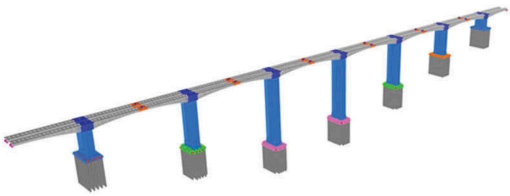

Figure 16. F.E. Model of the bridge in the project configuration with viscous damper devices.

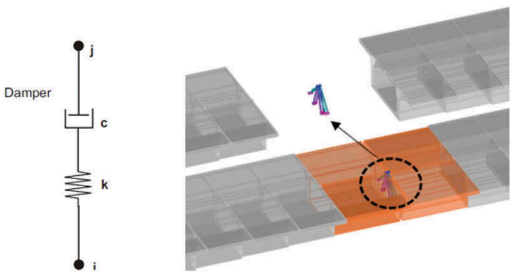

Figure 17. Model of exponential Maxwell damper links.

links are characterized by a linear spring in series with a non-linear damper, that represents the elasticity of the system, due to the compressibility of the fluid, and the damper contribution, respectively. The exponent α identifies the non-linearity of the response as a function of the velocity.

As a result of the strongly non-linear performance of the viscous dampers and the piers as well, the dynamic response of the structure is estimated by carrying out dynamic non-linear analyses with direct integration. Seismic input is applied by displacements time history with a duration equal to 20 s in the three directions of the seismic action and characterized by 8000 steps of 0,0025 s.

Due to the considerable span of the decks, spatial variability of the seismic motion is needed to be considered [5], which required the application of asynchronous time histories at the base of each pier of the bridge.

The asynchronous motion is commonly divided into three components [2]; [3]; [4]:

- wave passage effect;
- geometric incoherence of the input;
- local site conditions.

These three levels of incoherence are related to the ground motion coherency function proposed by Luco e Wong (1986):

$\gamma(\xi) = \exp[-(\alpha\omega\xi/v_s)^2] \exp[i (\omega\xi^L)/v_{app}]$

where α includes the mechanical characteristics of the soil; ξ and ξ^L = separation distance between two support points and the projected distance from the source, respectively; v_s = shear wave velocity; v_{app} = apparent surface wave velocity.

The first variable input quantity is the lumped shear wave velocity and soil property term v_s/α. This quantity controls the first term of the coherency function, and accounts for the geometric incoherence of the ground motion. The second input quantity v_{app} is the apparent surface velocity.

Setting $v_{app}=\infty$ is equivalent to an earthquake in which the seismic waves travel with infinite speed, reaching all bridge supports simultaneously, and making the motion coherent with regard to this parameter. On the other hand, when, we set $v_{app}=\infty$ and $v_s/\alpha=\infty$ the ground motion is perfectly synchronous.

Table 4 shows all ranges of coherency cases with their abbreviations to facilitate easy reference.

The level of geometric incoherence increases from left to right in the table, while wave passage severity increases from top to bottom. Thus, the upper left entry "in-in" corresponds to synchronous input motion, while the bottom right "30-30" represents the most incoherent case, with v_s/α and v_{app} values of 300 m/s.

In Table 5 ground motion cases considered in the seismic analyses carried out for the seismic retrofitting project of the bridge are detailed.

Table 4. Scheme of coherency cases and their abbreviations.

v_{app}	Infinity	v_s/α (inf-300)	300
Infinity	inf-inf	…	inf-30
(Infinity; 300)	…	…	…
300	30-30	…	30-30

For each ground motion and sources (7 piers and 2 abutments) and considering the maximum values of the effects raised from the analyses, no. 3 generation spectrum-compatible time histories are determined.

Table 5. Coherency cases considered in the seismic retrofitting project of the bridge.

Ground Motion	Type	v_{app}	v_s/α
1	asynchronous	1000	720
2	asynchronous	2000	720
3	asynchronous	1000	1140
4	asynchronous	2000	1140
5	asynchronous	1800	540
6	asynchronous	1800	1900
7	asynchronous	1800	inf
8	synchronous	inf	inf

As an example, Figures 18 and 19 show the displacements time histories for two among the eight cases of ground motion: inf-1800 (motion 7) and 540-1800 (motion 5). Figure 20 shows one of the spectrum-compatibility tests of the generated time histories.

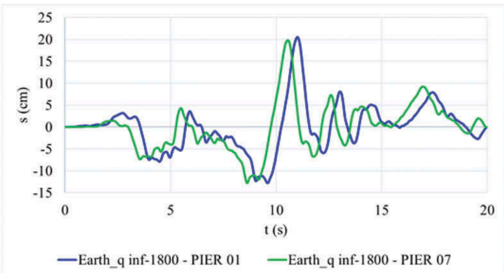

Figure 18. Displacements time histories for ground motion inf-1800.

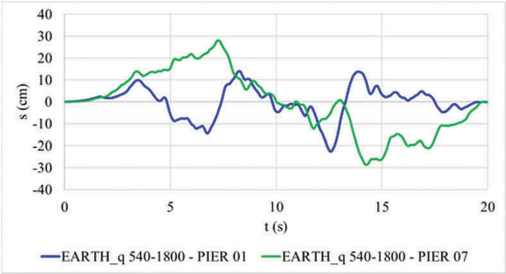

Figure 19. Displacements time histories for ground motion inf-540-1800.

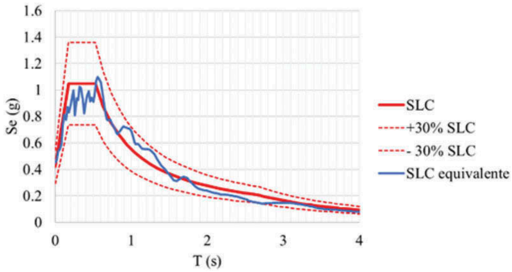

Figure 20. Spectrum-compatibility tests of generic time history.

5 RESULTS

5.1 *Hysteresis loop of viscous dampers*

With regard to the three types of viscous dampers installed into the bridge (1500; 2000; 2500), the relevant hysteresis loops related to the ground motion condition 5 (v_s/α=540; v_{app}=1800) are shown in following Figures 21, 22 and 23. It is noted that the ground motion condition no. 5 is one of the most severe overall.

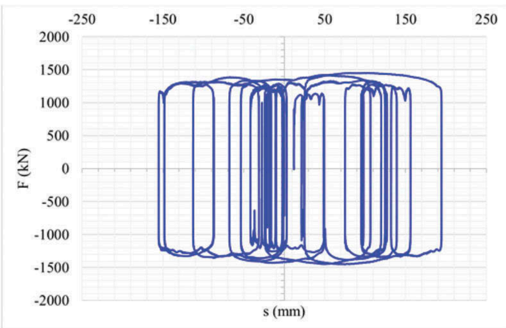

Figure 21. Hysteresis Loop of viscous dampers target force 1500 installed into the joint no. 1 (ground motion condition 540-1800).

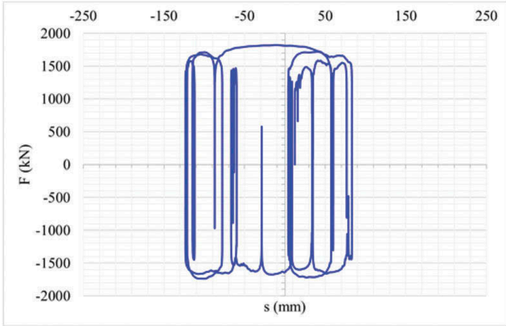

Figure 22. Hysteresis Loop of viscous dampers target force 2000 installed into the joint no.3 (ground motion condition 540-1800).

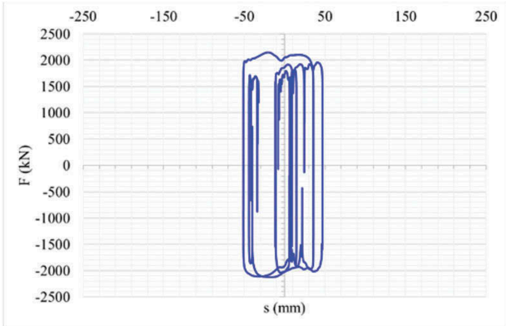

Figure 23. Hysteresis Loop of viscous dampers target force 2500 installed into the joint no.5 (ground motion condition 540-1800).

5.2 *Joints excursions in the post-operam*

The maximum and minimum excursions determined from the analyses with viscous dampers, for all the bridge joints and the ground motion conditions, are shown in Figure 24.

Table 6 shows the numerical values of the maximum and minimum excursions.

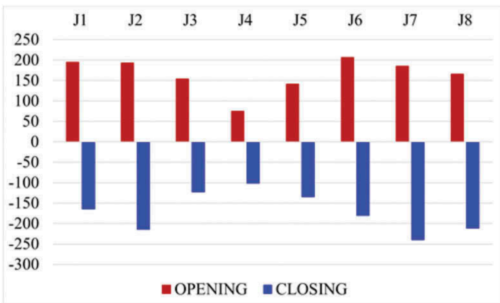

Figure 24. Joints Excursions (mm).

Table 6. Maximum and minimum excursions of the joints for each ground motion condition.

			GROUND MOTION							
		step	1	2	3	4	5	6	7	8
JOINT	1	max	136	178	99	122	194	82	88	61
		min	-130	-164	-78	-127	-157	-52	-77	-34
	2	max	193	144	71	47	134	55	57	119
		min	-215	-199	-112	-127	-168	-133	-137	-155
	3	max	122	154	109	93	98	76	59	47
		min	-80	-82	-78	-86	-123	-34	-38	-28
	4	max	22	62	29	20	75	16	19	-4
		min	-63	-102	-48	-67	-51	-45	-23	-8
	5	max	71	109	62	78	141	67	43	10
		min	-103	-70	-50	-76	-134	-68	-97	-19
	6	max	207	126	186	170	157	123	165	80
		min	-152	-166	-126	-180	-147	-70	-159	-103
	7	max	117	127	185	106	130	94	137	82
		min	-201	-221	-128	-240	-171	-136	-147	-91
	8	max	144	166	95	130	149	99	57	26
		min	-212	-165	-112	-125	-186	-66	-60	-17

5.3 *Comparison of joint excursions in ante-operam vs post-operam configuration.*

Table 7. Numerical comparison of maximum excursions between ante-operam (without v-damper) and post-operam (with v-damper) configuration.

JOINT	Without v-damper Δ (mm)	With v-damper Δ (mm)	Ratio with/ without -
1: ABUTMENT - PIER 1	254	194	0,77
2: PIER 1- PIER 2	485	215	0,44
3: PIER 2- PIER 3	674	154	0,23
4: PIER 3- PIER 4	776	102	0,13
5: PIER 4- PIER 5	707	141	0,20
6: PIER 5- PIER 6	549	207	0,38
7: PIER 6- PIER 7	416	240	0,58
8: PIER 7-ABUTMENT	236	212	0,90

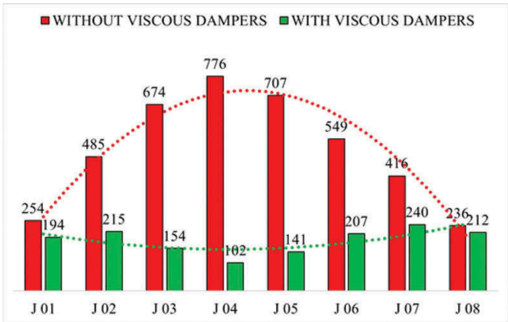

Figure 25. Graphical comparison of maximum excursions between ante-operam (without v-damper) and post-operam (with v-damper) configuration.

5.4 *Safety factors of piers*

Numerical and graphical results of the safety checks for all the piers of the bridge are summarized in Table 8.

Table 8. Minimum safety factors for shear and bending moments of piers.

PIER	Shear FS	Bending Moment FS
1	0,88>0,8	0,96>0,8
2	1,10>0,8	1,03>0,8
3	1,83>0,8	1,11>0,8
4	1,63>0,8	1,19>0,8
5	1,15>0,8	1,01>0,8
6	0,93>0,8	0,93>0,8
7	0,83>0,8	0,90>0,8

6 CONCLUSIONS

This work shows the retrofitting project of an Italian cantilever bridge realized with viscous damper devices.

The use of viscous dampers devices has allowed to improve the seismic response of the bridge and to obtain the safety factors required by Italian technical standards [8]. In particular, the use of such viscous dampers has made it possible to overcome the main criticality, emerged from the assessment of the seismic response in the original configuration, which is the maximum capacity of the shear keys' excursion interposed between the spans.

On the bases of the analysis carried out and detailed in this work, we can point out the positive effects of viscous dampers devices used in this project below:

a. Dynamic response of bridge in *post-operam* configuration is substantially different from that of the *ante-operam*. The viscous dampers devices allow the 7 piers and the decks to interact; consequently, the stresses and relative displacements are balanced. The safety factors of the structures are suitable in accordance with the objectives set;
b. The maximum excursions of the bridge expansion joint for each ground motion case – *synchronous and asynchronous* – are lower than the excursion capacity of the new shear keys (300 mm) and, therefore, of the new joints' width (320 mm). It is possible to conclude that the risk of loosening of the shear keys and the pounding effect of the decks, should be excluded with the installation of viscous dampers;
c. The optimized system configuration of the viscous dampers, calibrated with damping capacity inversely proportional to the stiffness of the piles, confers substantial benefits to the structure. This configuration allows to limit the displacements of the highest and most flexible piers and to limit the shear stresses in the more rigid piers, characterized by lower natural frequencies, at the same time. The ratios between the excursions of the internal joints (2-7), obtained from the *post-operam* and *ante-operam* configuration, are variable between 0.13 for the highest piers and 0.44 for those ones lower, accordingly to the project strategy of dissipation system;
d. The maximum stresses induced by the seismic action in the piers are compatible with the relative capacity. The shear and bending moments safety checks are all satisfied. The minimum safety factors are equal to 0,88 and 0,93 for the shear and bending moment, respectively. These values are greater than 0,8, which is the minimum value required by Italian technical standards. Therefore, the seismic retrofitting of the bridge shall be deemed successful.

REFERENCES

[1] Sleemah, A.A.; Constantinou, M.C., *"Investigation of Seismic Response of Structures of Buildings with Linear and Nonlinear Fluid Viscous Dampers"*. Tech Rep. NCEER-97-0004, National Centre for Earthquake Engineering. Research, State Univ. of NewYork (SUNY) at Buffalo, NY, (1997).

[2] Lupoi, A., Franchin, P., Pinto, P.E., Monti, G., *Seismic design of bridges accounting for spatial variability of ground motion*. Earthq. Eng. Struct. Dyn, **34** (4-5):327–348, (2005).

[3] Burdette, N.J., Elnashai, A.S., Lupoi, A., Sextos, A.G., *"The Effect of Asynchronous Earthquake Motion on Complex Bridges"*. ASCE J. Bridge Engrg. **13**(2): 158–165. DOI: 10.1061/(ASCE)1084-0702(2008)13:2(158). WOS:000253392400005. ISSN: 1084-0702, (2005).

[4] Lupoi, A., *"Seismic Response of Isolated bridges accounting for spatial variability of ground motion"*. Journal of Earthquake Engineering, **13**(6): 814–834. DOI: 10.1080/13632460802645106. WOS:000268033100004. ISSN: 1363-2469, (2009).

[5] Bodganoff, J. L., Goldberg, J. E., and Schiff, A. J., *"The effect of ground transmission time on the response of long structures."* Bull. Seismol. Soc. Am., 55, 627–640, (1965).

[6] Zienkiewicz O.C., Taylor R.L., *"The finite element method"*. McGraw Hill, Vol. I., 1989, Vol. II, (1991).

[7] S. Idelsohn and E. Oñate, *"Finite element and finite volumes. Two good friends"*. Int. J. Num. Meth. Engng, 37, 3323–3341, (1994).

[8] D.M. 17/01/2018 – *Aggiornamento delle "Norme Tecniche per le Costruzioni"*. Ministero delle Infrastrutture e dei Trasporti.